Preparation and characterization of $Ce_{0.3}Ti_{0.7}O_2$ and supported CuO catalysts for NO + CO reaction

Xiaoyuan Jiang[a,*], Liping Lou[b], Yingxu Chen[b], and Xiaoming Zheng[a]

[a]*Institute of Catalysis, Zhejiang University, Hangzhou 310028, P.R. China*
[b]*Department of Environmental Engineering, Zhejiang University, Hangzhou 310028, P.R. China*

Received 27 August 2003; accepted 28 January 2004

The $Ce_xTi_{1-x}O_2$ mixed oxides at different mole ratios ($x = 0.1$–1.0) were prepared by co-precipitation of $TiCl_4$ and $Ce(NO_3)_3$. The structural and reductive properties of the $Ce_xTi_{1-x}O_2$ were affected by calcination temperature. At $x = 0.1$–0.3, $CeTi_2O_6$ phase was formed and mainly as amorphous after calcination at 650 °C. At $x = 0.3$, only $CeTi_2O_6$ was formed after calcination at 750 °C and $CeTi_2O_6$ crystallized completely after calcination at 800 °C. TPR analyses showed that the amount of H_2 consumption by $Ce_xTi_{1-x}O_2$ (650 °C) (except $x = 0.1$) was greater than that by single CeO_2, and the valence of CeO_2 was the lowest (+3.18) at $x = 0.3$. $CuO/Ce_{0.3}Ti_{0.7}O_2$ was prepared by the impregnation method and catalytic properties were examined by means of a GC micro-reactor NO + CO reaction system, BET, TPR, XRD, XPS and NO-TPD. It was found that $CuO/Ce_{0.3}Ti_{0.7}O_2$ calcined at 650 °C had the highest activity in NO + CO reaction with 100% NO conversion at reaction temperature of 300 °C, and at 650 °C $Ce_{0.3}Ti_{0.7}O_2$ just began to crystallize. The catalytic activities were largely affected by the pre-treatment conditions. At low reduction temperature (100 °C), CuO species was difficult to reduce. When high degree of reductions took place, both CuO species and $Ce_{0.3}Ti_{0.7}O_2$ reduced and thus a part of CuO species on the support surface would be covered. The XPS and NO-TPD analyses showed that $CuO/Ce_{0.3}Ti_{0.7}O_2$ had four NO absorption centers (Cu^+, Cu^{2+}(I), Cu^{2+}(II) and Ce^{3+}). The CuO species involving in NO + CO reaction included Cu^{2+}(I) and Cu^+, and CeO_2 species (Ce^{3+} and Ce^{4+}).

KEY WORDS: $Ce_{0.3}Ti_{0.7}O_2$; $CeTi_2O_6$ phase; $CuO/Ce_{0.3}Ti_{0.7}O_2$ catalysts; NO + CO reaction.

1. Introduction

From 1980's, CeO_2 has been widely used in purifying vehicle exhausts and become the most important rare earth oxides for controlling NO_x. CeO_2 increases the dispersion of active components and thermal stability of the support, and enhances the migration and exchange of oxygen species in reactions by storing and releasing oxygen of CeO_2 so as to improve CO, HC oxidation and NO_x reduction [1,2]. The Ce^{3+}/Ce^{4+} redox cycle also leads to high catalytic activity of CeO_2. However, since single CeO_2 would be sintered after calcination at 750 °C [3], some mixed oxides or solid solutions (e.g. CeO_2–ZrO_2) were prepared by adding anti-sintered oxides [4–8]. In the solid solution of CeO_2–ZrO_2, the replacement of some Ce atoms by other cations led to the micro-stain and lattice defect of CeO_2 and thus better catalytic activity in low temperatures, thermal stability and higher redox potential than single CeO_2 [4–8]. In recent years, besides CeO_2–ZrO_2, much attention has been paid to the preparation and characterization of such mixed oxides as CeO_2–SnO_2 [9], CeO_2–TiO_2 [10–12], and CeO_2–NiO [13]. For example, the $Ce_xTi_{1-x}O_2$ mixed oxides were prepared using the sol–gel methods with the raw materials of inorganic Ce salt and titanium alcohol salt [10–12]. The Ce and Ti ions have several valences and their mixed oxides thus have very complex chemical valences and molecular formula. Until now, $CeTi_2O_6$ is the only known Ce–Ti mixed oxide in a form of Ce^{4+} and Ti^{4+}. By comparison, most of studies have found the Ce–Ti mixed oxides in a form of Ce^{3+} and Ti^{4+}, e.g. Ce_2TiO_5, $Ce_2Ti_2O_7$ and $Ce_4Ti_9O_{24}$ by Pruess and Gruehn [14], and $Ce_2Ti_4O_{11}$ by Bamger *et al.* [15]. Dauscher *et al.* [16] used organic titanium alcohol salt and $CeCl_3$–$7H_2O$ to prepare Ce-Ti mixed oxides of Ce/Ti = 1 with the method of hydrolytic dryness. In this study, $Ce_xTi_{1-x}O_2$ composite oxides were prepared by co-precipitation, and the effects of CuO loading on the $Ce_xTi_{1-x}O_2$ structures and catalytic activities in NO + CO reaction were examined by means of BET, TPR, XRD, XPS and NO-TPD.

2. Experimental

2.1. The preparation of $Ce_xTi_{1-x}O_2$

$Ce_xTi_{1-x}O_2$ was prepared by co-precipitation method. Aqueous solutions of $TiCl_4$ and $Ce(NO_3)_3$–$6H_2O$ at a desired proportion were well mixed and dripped into concentrated aqua ammonia (pH = 11.0). After being laid for 24 h, the mixtures were washed to clean Cl^- and dried at 50 °C, and then calcined in an air stream at 650, 750 and 800 °C for 2 h, respectively.

2.2. Catalysts preparation

Using $Ce_xTi_{1-x}O_2$ as a support, the $CuO/Ce_{0.3}Ti_{0.7}O_2$ catalysts were prepared by the impregnation method

* To whom correspondence should be addressed.
E-mail: xyjiang@mail.hz.zj.cn

1011-372X/04/0400–0049/0 © 2004 Plenum Publishing Corporation

using $Cu(NO_3)_2$ aqueous solutions at desired concentrations. The catalysts were dried for 12 h and then calcined in an air stream at 500 °C for 2 h, and denoted as (wt%) $CuO/Ce_xTi_{1-x}O_2$.

2.3. Measurements of catalytic activity in NO + CO reaction

Catalytic activity was measured under the steady state in a fixed-bed quarta reactor at a space velocity of 5000 h. The reaction gas consisted of a fixed composition of 6.0% NO, 6.0% CO and 88% He (v/v). Two columns and thermal conduction detectors were used to measure the catalytic activity. Column A was packed with 13× molecular sieve for separating N_2, NO and CO, and column B was packed with Porapak Q for separating N_2O and CO_2. The temperature of two columns was 55 °C and the flow rate of H_2 was 30 mL/min.

2.4. Measurements of catalytic properties

The BET specific surface area of catalysts and pore size were determined by N_2 adsorption at 77 K using a Coulter OMNISORP-100 instrument.

H_2-temperature-programmed reduction (TPR) was done by gas chromatography (GC) using a thermal conductivity detector. The sample (5–10 mg) was activated in an O_2 stream at 500 °C for 0.5 h. After cooled down to 30 °C, the H_2-TPR was conducted.

X-ray diffraction (XRD) data were obtained using a horizontal Rigaku B/Max IIIB powder diffractometer with CuK_α radiation and a power of 40 kV × 40 mA.

X-ray photoelectron spectra (XPS) were recorded by PHI-5000C ESCA spectrometer with AlK_α radiation of 1486.6 eV and MgK_α radiation of 1253.6 eV. The calibration of the spectrometer energy scale was performed using silver (Ag $3d_{5/2} = 4 \times 10^{-4}$ cps). The C_{1s} line at 284.6 eV was used as an internal standard for the correction of binding energies.

For measuring the NO-temperature-programmed desorption (TPD), 250 mg of fresh catalysts were loaded onto a quartz reactor and treated in $10\%CO/N_2$ or $6\%NO + 6\%CO$ atmosphere at 500 °C for 0.5 h. The catalysts were then heated in He at 600 °C for 1 h, cooled to 40 °C in a flow of He and exposed to 10%NO–He mixture gas. Excessive NO was removed and the catalysts were kept in He flow until no significant amount of adsorbates could be detected. The catalysts were then ramped at 800 °C at a linear heating rate of 20 °C/min. The effluent gases were analyzed with a mass spectrometer.

3. Results and discussion

3.1. Analysis of crystal phase of $Ce_xTi_{1-x}O_2$

The XRD patterns of $Ce_xTi_{1-x}O_2$ calcined at 650 °C with different mole ratios are shown in figure 1. At $x = 0$, TiO_2 existed as anatase and rutile. At $x = 0.1$, small amount of rutile besides $CeTi_2O_6$ was detected. At $x = 0.2$, several diffraction peaks of rutile and $CeTi_2O_6$ were observed. At $x = 0.3$, $Ce_xTi_{1-x}O_2$ was mostly amorphous. A diffraction peak of CeO_2 was observed at $x = 0.4$–1.0. At $x = 1.0$, CeO_2 existed as cubic phase and the diffraction peak was very sharp and thin. By comparison, the diffraction peaks of other samples were smoother and changed in relation with x values. The results indicated that a rich-cerium solid solution was formed and it had the same cubic phase as CeO_2. When x values increased from 0.4 to1.0, the d value of the strongest diffraction peak of $Ce_xTi_{1-x}O_2$ increased from 3.0932 to 3.1293. This was because the ion radius of Ce^{4+}(0.094 nm) is larger than Ti^{4+}(0.068 nm) and the amount of Ce^{4+} in solid solutions continued to increase.

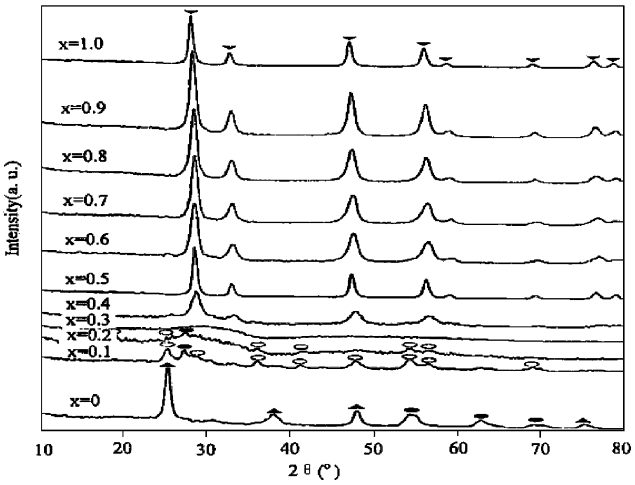

Figure 1. XRD patterns of $Ce_xTi_{1-x}O_2$ (650 °C) samples. (▼) CeO_2; (▲) Anatase; (●) Rutile; (○) $CeTi_2O_6$.

Figure 2 shows the XRD patterns of $Ce_xTi_{1-x}O_2$ with different mole ratios calcined at 750 and 800 °C respectively. $CeTi_2O_6$ largely crystallized after calcination at 750 °C, and all the $CeTi_2O_6$ had crystallized after calcination temperature rose to 800 °C. At $x < 0.3$, CeO_2 and rutile were detected besides $CeTi_2O_6$. At $x = 0.3$, CeO_2 and TiO_2 disappeared. At $x = 0.4$ or 0.5, both CeO_2 and $CeTi_2O_6$ existed, and little $CeTi_2O_6$ was detected at $x = 0.6$. Rynkowski *et al.* [10] prepared CeO_2–TiO_2 at an atom radio of Ce/Ti of 2:8 or 5:5 using *n*-butyl tianate–cerium nitrate solution as raw material by the sol–gel method and found an unknown compound, which had a XRD pattern similar to that we detected. This compound was likely to be $CeTi_2O_6$. At $x > 0.6$, the catalytic activity was not obviously related to the calcination temperature and CeO_2 was detected by XRD, indicating that TiO_2 entered into the crystal lattice of CeO_2.

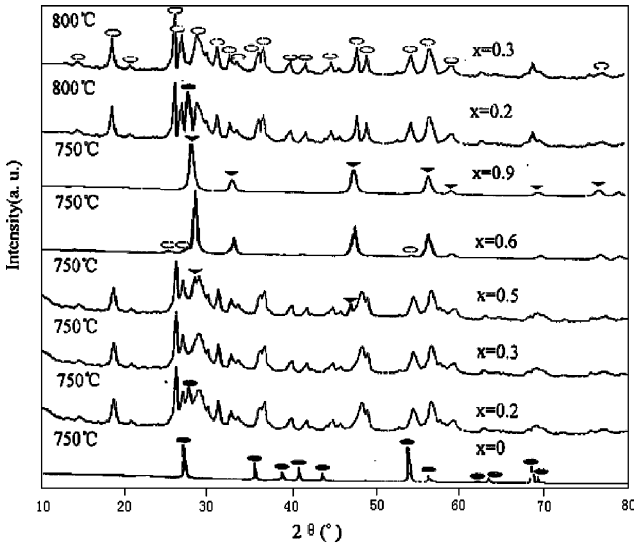

Figure 2. XRD patterns of $Ce_xTi_{1-x}O_2$ (750 and 800 °C) samples (▼) CeO_2; (●) Rutile; (○) $CeTi_2O_6$.

3.2. H_2 consumption of $Ce_xTi_{1-x}O_2$ and the reduction degree of CeO_2 in $Ce_xTi_{1-x}O_2$

It was presumed that only component CeO_2 can be reduced. The reduction of CeO_2 in $Ce_xTi_{1-x}O_2$ was estimated by the H_2 consumption of $Ce_xTi_{1-x}O_2$ and molecular weight. As shown in table 1, the H_2 consumption of $Ce_xTi_{1-x}O_2$ calcined at 650 °C was much greater than that of single CeO_2 except the case of $x = 0.1$, meaning that addition of TiO_2 increased the reduction of CeO_2. The existence of Ti^{4+} in $Ce_xTi_{1-x}O_2$ calcined at 650 °C might weaken the Ce–O bond and result in CeO_2 reduction more easily. In the reduction of $Ce_xTi_{1-x}O_2$, the valence state of Ce was the lowest (+3.18) at $x = 0.3$ and lower than +3.5 at $x = 0.2$–0.6, compared to +3.85 of pure CeO_2, indicating that the $Ce_xTi_{1-x}O_2$ mixed oxides were an agent of storing oxygen. After $Ce_xTi_{1-x}O_2$ was calcined at 800 °C, the decrease in specific surface area caused less H_2 consumption (table 2). At $x = 0.3$ and 0.4, however, H_2 consumption increased with the increase in calcination temperature. This did not mean $Ce_{0.3}Ti_{0.7}O_2$ and $Ce_{0.4}Ti_{0.6}O_2$ were easily reduced after calcination at 800 °C. It was likely that the valence of CeO_2 was not +4 in $Ce_xTi_{1-x}O_2$ calcined at 650 °C but changed to +4 in $Ce_xTi_{1-x}O_2$ calcined at 800 °C. Namely, $Ce_xTi_{1-x}O_2$ adsorbed oxygen during calcination at 800 °C, which led to an increase in H_2 consumption by the mixed oxides.

3.3. BET specific surface area of $Ce_{0.3}Ti_{0.7}O_2$

The BET specific surface area of $Ce_{0.3}Ti_{0.7}O_2$ after calcination at 500 °C was 207.3 m^2/g and decreased sharply to 58.7 m^2/g after calcination at 650 °C, but it slowly decreased with further increase in calcination temperature and was 44.6 m^2/g at 800 °C (table 2).

3.4. The activity of $CuO/Ce_{0.3}Ti_{0.7}O_2$ in NO + CO reaction

The activity of $Ce_{0.3}Ti_{0.7}O_2$ calcined at 650 °C was affected by the amount of CuO loading (figure 3). At reaction temperature of 500 °C, the activity of $Ce_{0.3}Ti_{0.7}O_2$ was quite low and the NO conversion was only 43% but the NO conversion increased to 93% at 1% CuO loading, and appeared the waves of activity with a plateau or even a decrease in between at reaction temperature of 250–300 °C. Further increase in CuO loading caused the waves of activity moving toward the direction of low temperature. The activities of

Table 2
Specific surface area of $Ce_{0.3}Ti_{0.7}O_2$ with different calcination temperatures

Calcination temperature (°C)	500	650	750	800
Specific surface area (m^2/g)	207.3	58.7	50.2	44.6

Table 1
H_2 consumption of $Ce_xTi_{1-x}O_2$ and the reduction of CeO_2 in $Ce_xTi_{1-x}O_2$

Mole ratios	H_2 consumption (mmol/g)		Composition of reduced sample			
(x)	(650 °C)	(800 °C)	y in $Ce_xTi_{1-x}O_y$ (650 °C)	y in $Ce_xTi_{1-x}O_y$ (800 °C)	Valence of CeO_2 (650 °C)	Valence of CeO_2 (800 °C)
0.1	0.3252	0.0837	1.9710	1.9225	3.42	3.85
0.2	0.4974	0.4667	1.9511	1.9541	3.51	3.54
0.3	1.1478	1.4428	1.8766	1.8449	3.18	2.97
0.4	1.0840	1.5514	1.8735	1.8189	3.37	3.09
0.5	1.1861	0.3154	1.8506	1.9603	3.40	3.84
0.6	1.3455	0.2253	1.8181	1.9695	3.39	3.90
0.7	0.9438	0.2092	1.8637	1.9698	3.61	3.91
0.8	0.9182	0.2446	1.8589	1.9624	3.65	3.91
0.9	0.8162	0.1384	1.8670	1.9775	3.70	3.95
1.0	0.4336	0.1030	1.9254	1.9823	3.85	3.96

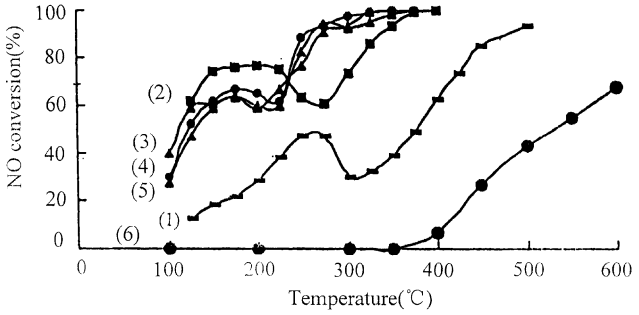

Figure 3. Effect of CuO loading on the activity of $Ce_{0.3}Ti_{0.7}O_2$ (650 °C) in NO + CO reaction; (1) 1%CuO/$Ce_{0.3}Ti_{0.7}O_2$; (2) 3%CuO/$Ce_{0.3}Ti_{0.7}O_2$; (3) 6%CuO/$Ce_{0.3}Ti_{0.7}O_2$; (4) 12%CuO/$Ce_{0.3}Ti_{0.7}O_2$; (5) 18%CuO/$Ce_{0.3}Ti_{0.7}O_2$; (6) $Ce_{0.3}Ti_{0.7}O_2$.

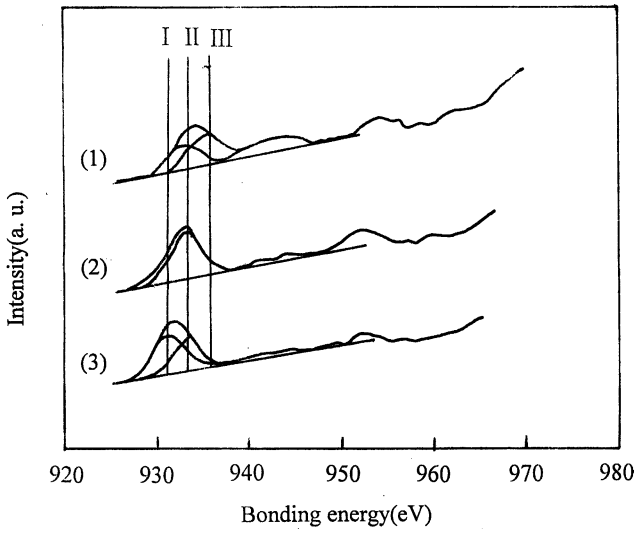

Figure 4. Bonding energy of $Cu2P_{3/2}$ of 6%CuO/$Ce_{0.3}Ti_{0.7}O_2$ samples with different pre-treatments. (1) Fresh catalysts; (2) Pre-reduced by reaction gases (6%NO + 6%CO); (3) Pre-reduced by 10%CO/N_2 at 200 °C.

$CuO/Ce_{0.3}Ti_{0.7}O_2$ were similar at 6% and 12% CuO loading, and the NO conversion reached 100% at 300 °C. Further increase in CuO loading caused a decrease in catalytic activities because CuO gathered at the surface of the supports.

The appearance of waves of activity with a plateau or even a decrease in between from 6%CuO/$Ce_{0.3}Ti_{0.7}O_2$ (calcined at 650 °C) was examined by conducting re-reaction. Through the re-reaction, catalytic activity increased with increase in reaction temperature and the waves of activity disappeared at 175–300 °C. Compared with the original activity, the re-reaction activity decreased slightly at <200 °C but increased at >200 °C. The activity of the third-time reaction was similar to that of the second-time reaction, indicating that the surface state of the catalyst was stabilized during the first-time reaction. When the catalyst was re-activated by calcination in an air stream at 500 °C for 2 h, the plateau activity re-appeared at 175–300 °C. We presumed that the phenomenon could be due to the effect of reaction gases (6%NO + 6%CO) on CuO and CeO_2 and changes of the dispersion state of the active components. The findings of no waves of activity with a plateau or even a decrease in between when the catalyst was pre-treated with 10%CO/N_2 at 200 °C for 2 h also provided evidence of our presumption. Monte *et al.* [17] studied the activity of Pd/CeO_2–ZrO_2 catalyst by means of XANES in site and found the plateau activity or even a decrease in-between at 500–600 K, and suggested that the phenomenon may be the oxidation function of part of CeO_2.

3.5. Analysis of XPS

Samples with different pre-treatments were analyzed by XPS for reaction mechanism and catalyst surface species in the NO + CO reaction. table 3 shows the bonding energy of $Cu2p_{3/2}$ of 6%CuO/$Ce_{0.3}Ti_{0.7}O_2$. As shown in table 3 and figure 4, two forms of CuO existed on the support with the binding energies of 933.29 and 935.20 eV, representing CuO and –Cu–O–Ti–O– [18] and recorded as Cu^{2+}(I) and Cu^{2+}(II), respectively. However, the peak of bonding energy of $Cu2P_{3/2}$ at 935.20 eV disappeared after pre-treatment with 6%NO + 6%CO gas, despite a small peak at 931.40 eV that represented Cu^0 or Cu^+. At this time, the Cu species mainly existed as Cu^{2+}(I)(86.3%). The disappearance of the peak at 935.20 eV indicated that this peak was unstable but had high activity. By comparison, after pre-treatment with 10%CO at 200 °C, the Cu species were mainly Cu^0 or Cu^+ (74%) plus Cu^{2+}(I) (26%), and after pre-treatment with pure H_2 at 400 °C, the Cu species were mainly Cu^0 or Cu^+(89%) plus Cu^{2+}(I) (11%).

Table 4 shows the bonding energy and atomic ratio of 6%CuO/$Ce_{0.3}Ti_{0.7}O_2$ with different pre-treatments. The atom ratio of Ce/Ti was 1.248 in the fresh

Table 3
Bonding energy of $Cu2p_{3/2}$ of 6%CuO/$Ce_{0.3}Ti_{0.7}O_2$ with different pre-treatment

Cu species	Fresh BE (eV)	Proportion (%)	T1[a] BE (eV)	Proportion (%)	T2[b] BE (eV)	Proportion (%)
Cu^+	–	–	931.4	13.7	931.2	74
Cu^{2+}(I)	933.29	47.6	932.97	86.3	932.91	26
Cu^{2+}(II)	935.2	52.4	–	–	–	–

[a]Treatment 1: treated using by 6%NO + 6%CO reaction gases at 300 °C for 1 h.
[b]Treatment 2: treated using by 10%CO/N2 at 200 °C for 1 h.

Table 4
Bonding energy and atomic ratio of 6%$CuO/Ce_{0.3}Ti_{0.7}O_2$ with different pre-treatment

–	$Ce_{0.3}Ti_{0.7}O_2$ Fresh	6%$CuO/Ce_{0.3}Ti_{0.7}O_2$ Fresh	6%$CuO/Ce_{0.3}Ti_{0.7}O_2$ T1[a]	6%$CuO/Ce_{0.3}Ti_{0.7}O_2$ T2[b]
$Ce_{3d3/2}$	882.86	882.89	882.07	882.01
$Ti_{2p3/2}$	458.7	459.2	458.3	458.3
$O1s_{lattice}$	529.5	530.0	529.8	529.7
Ce/Ti	1.248	1.085	1.168	1.123
Cu/(Ti + Ce)	–	0.131	0.148	0.141
Cu/Ce	–	0.253	0.275	0.267
Cu/Ti	–	0.270	0.32	0.30
U'''/I_{total}	0.269	0.263	0.113	0.102
Ce^{3+}(%)	0.178	0.245	0.29	0.306

$Ce_{0.3}Ti_{0.7}O_2$ and decreased to 1.085 after CuO loading. Moderate reactions and reduction conditions contributed to the dispersion of active components on the surface and so an increase in the atom ratio of Cu/(Ce + Ti) from 0.131 to 0.148 and 0.141 on the fresh catalysts. Under H_2 reduction, the amount of dispersed Cu species on the surface decreased dramatically and the ratio of Cu/(Ce + Ti) was only 0.053. A large decrease in the Cu/Ti and Cu/Ce ratios was also observed, whereas the ratio of Ce/Ti increased. Figure 8 also shows that the bonding energy peak of Cu $2P_{3/2}$ of 6% $CuO/Ce_{0.3}Ti_{0.7}O_2$ samples decreased with H_2 and was much less than other samples. The atom ratio of Cu/Ti of CuO/TiO_2 system under H_2 condition decreased slightly (from 0.39 to 0.32). The results suggested that the decrease in Cu/(Ce + Ti) ratio was due to the reduction of $Ce_{0.3}Ti_{0.7}O_2$, which overlapped Cu species on the surface. Therefore, the activity of catalysts reduced by CO was better than that by H_2. As the Ce/Ti ratio increased, the decrease in the Cu/Ce ratio was larger than that in Cu/Ti, indicating that the decrease in Cu species was likely the result of covering by Ce species. The XRD analysis found that during the reduction of 6% $CuO/Ce_{0.3}Ti_{0.7}O_2$ by H_2, $Ce_{0.3}Ti_{0.7}O_2$ partly dissociated into CeO_2 and TiO_2, which was responsible for covering the Cu species.

The $Ti2p_{3/2}$ binding energy of 6%$CuO/Ce_{0.3}Ti_{0.7}O_2$ with different pre-treatments was around 458–459 eV. However, the Ce3d spectral line showed eight XPS peaks and displayed the $Ce3d_{5/2}$–$Ce3d_{3/2}$ spin-orbit splitting (one doublet). The other peaks were the satellite structures of these principal peaks (figure 9). For the twin peaks of spin orbital, *u* usually represented the electron binding energy of $3d_{5/2}$ and *v* represented the electron binding energy of $3d_{3/2}$, and both valued between 875 and 925 eV [10,19]. The *v* of $3d_{3/2}$ level stood for the final state of $3d^94f^2(O2p^4)Ce(IV)$; *v*'' for that of $3d^94f^1(O2p^5)Ce(IV)$; *v*''' for that of $3d^94f^0(O2p^6)$-Ce(IV) and *v*' for that of $3d^94f^1(O2p^6)Ce(III)$. The meanings of *u* were similar to those of *v*, except that *u* stood for the binding energy of $3d_{5/2}$. The ratio of Ce^{4+}/Ce^{3+} determined the *u*''' intensity and its ratio of the total intensity (I_{total}). With the increase of Ce^{3+}, the ratio of u'''/I_{total} decreased but the ratio of $u' + v'/I_{total}$ increased.

The percentage of Ce^{3+} in all cerium was calculated as, Ce^{3+} (%) = 100%* (S*v*' + S*u*')/Σ(S*v* + S*u*). As shown in table 3, Ce^{3+} accounted for 17.8% of all surface Ce of the $Ce_{0.3}Ti_{0.7}O_2$ supports, which was lower than the number of earlier report [10]. After CuO loading, Ce^{3+} was equal to 24.5% of all surface Ce. After $CuO/Ce_{0.3}Ti_{0.7}O_2$ was reduced by 10%CO/N_2 and pure H_2, Ce^{3+} accounted for 30.6% and 42.9% of all surface Ce respectively. In contrast, the trend of u'''/I_{total} was opposite to that of Ce^{3+}. After reduction by H_2, the *u*''' and *v*''' peaks of $3d^94f^0(O2p^6)Ce(IV)$ disappeared. In addition, the Ce3d spectral line greatly increased as the

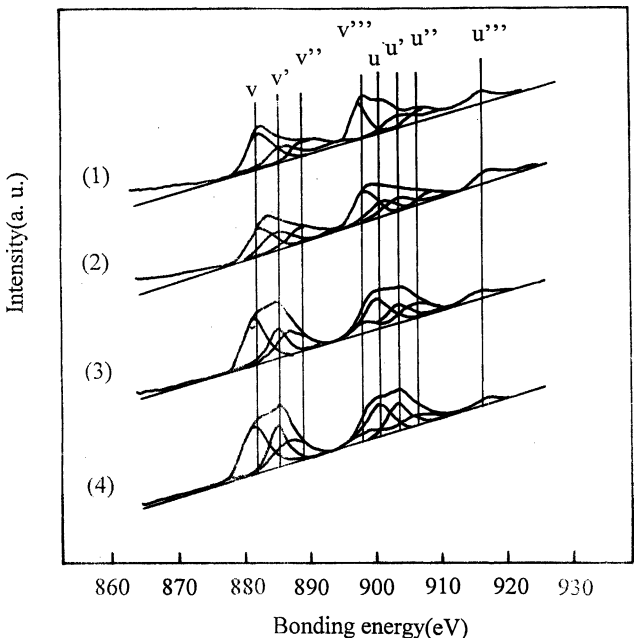

Figure 5. Bonding energy of $Ce_{3d5/2}$ of $Ce_{0.3}Ti_{0.7}O_2$ and 6%$CuO/Ce_{0.3}Ti_{0.7}O_2$ samples with different pre-treatments, $Ce_{0.3}Ti_{0.7}O_2$; (2) Fresh 6%$CuO/Ce_{0.3}Ti_{0.7}O_2$; (3) 6%$CuO/Ce_{0.3}Ti_{0.7}O_2$ treated with 6%NO + 6%CO; (4) 6%$CuO/Ce_{0.3}Ti_{0.7}O_2$ treated with 10%CO/N_2 at 200 °C.

degree of reduction increased (figure 9), indicating an enrichment of Ce species on the sample surface (figure 5).

3.6. NO-TPD detection

NO, N_2O and N_2 signals were detected in the NO-TPD processing of $CuO/Ce_{0.3}Ti_{0.7}O_2$ (figures 6–8). After the catalyst adsorbed NO, four absorbing sites were found by mass spectrometer tracking. Although $Ce_{0.3}Ti_{0.7}O_2$ absorbed large amount of NO, its NO dissociation activity was low. As a consequence, little N_2O and N_2 but large amount of O_2 was formed at 580 °C. Both O_2 and NO_2 were only detected in $CuO/Ce_{0.3}Ti_{0.7}O_2$ catalysts treated with He at 400 °C. It was likely that NO decomposition produced atomic oxygen (O) that entered into the reduced catalysts and the desorption of atomic oxygen could only occur at high temperatures [20]. The quantity of NO desorption was larger on $CuO/Ce_{0.3}Ti_{0.7}O_2$ than that on $Ce_{0.3}Ti_{0.7}O_2$, suggesting that NO was mainly absorbed on the CuO surface.

The thermal desorption products during NO-TPD processing were associated with the pre-treatment conditions. Five absorbing sites of NO on $CuO/Ce_{0.3}Ti_{0.7}O_2$ were examined in this study (table 5),

(1) S5 adsorbing site only existed in fresh samples. In accordance with the XPS results, this site might ascribe to Cu^{2+}(II).
(2) S4 and S3 sites were detected with different pre-treatments. In addition, S3 site was the largest after treatment 10%CO/N_2, while S4 site increased

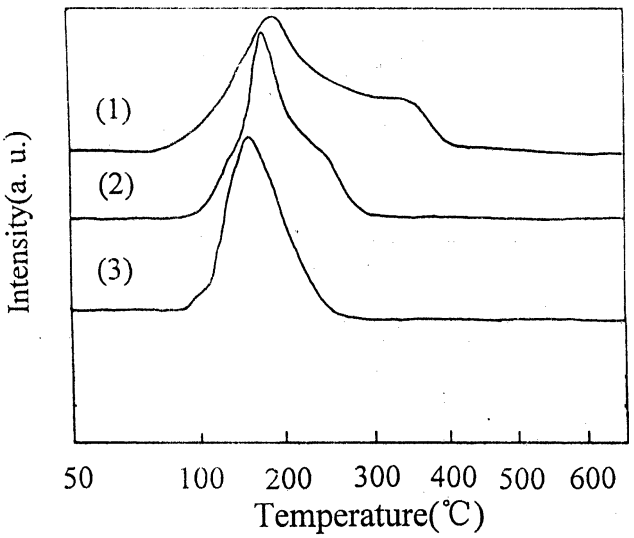

Figure 6. NO signal during NO-TPD processing of $CuO/Ce_{0.3}Ti_{0.7}O_2$ with different pre-treatments. (1) Treated with He at 400 °C; (2) Treated with 6%NO + 6%CO at 400 °C; (3) Treated with 10%CO/N_2 at 200 °C.

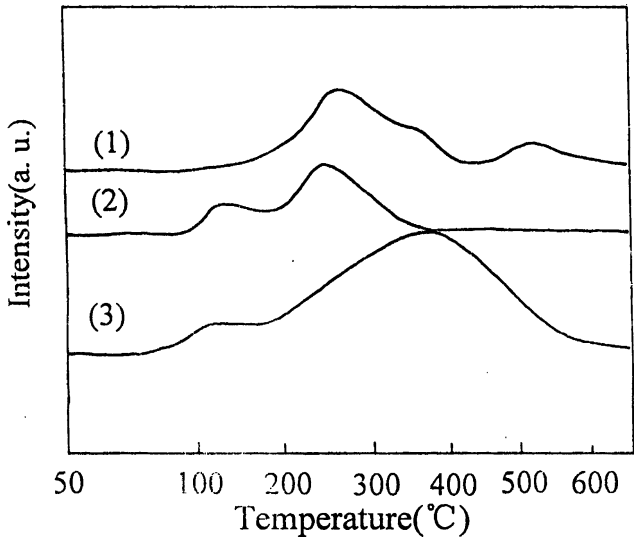

Figure 7. N_2O signal during NO-TPD processing of $CuO/Ce_{0.3}Ti_{0.7}O_2$ with different pre-treatments. (1) Treated with He at 400 °C; (2) Treated with 6%NO + 6%CO at 400 °C; (3) Treated with 10%CO/N_2 at 200 °C.

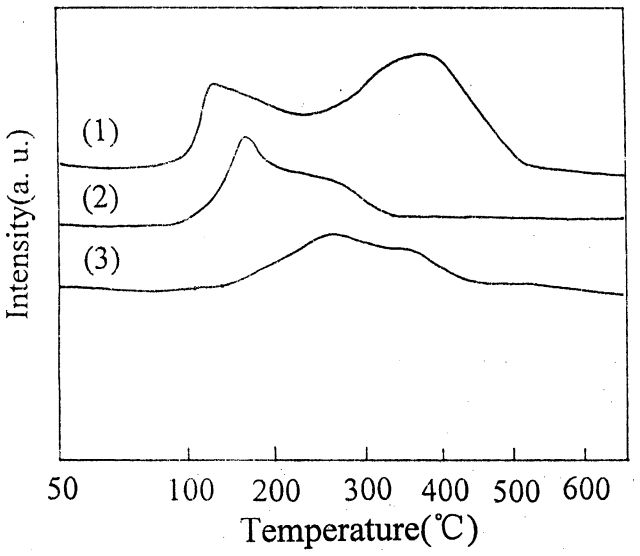

Figure 8. N_2 signal during NO-TPD processing of $CuO/Ce_{0.3}Ti_{0.7}O_2$ with different pre-treatments. (1) Treated with He at 400 °C; (2) Treated with 6%NO + 6%CO at 400 °C; (3) Treated with 10%CO/N_2 at 200 °C.

Table 5
Ascription of various absorbing site on CuO/Ce0.3Ti0.7O2 and its desorped species

Site	Temperature (°C)	Ascription	Desorped species
S1	100	Ce^{3+}	NO, N_2O, N_2
S2	115	Cu^0	NO, N_2O, N_2
S3	140	Cu^+	NO, N_2
S4	198	Cu^{2+}(I)	NO, N_2O, N_2
S5	280	Cu^{2+}(II)	NO, N_2O, N_2

with the oxidation extent of pre-treatment atmosphere. In accordance with the XPS results, they might ascribed to Cu^{2+}(I) and Cu^{+}.

(3) At both S1 and S2 sites, the peak areas, NO dissociation and N_2 desorption increased with the reduction extent of pre-treatment atmosphere. S2 site might ascribe to Cu^0 and S1 site to Ce^{3+}.

4. Conclusion

(1) At $x = 0.1$–0.3, the phase of $CeTi_2O_6$ formed after calcination at 650 °C and was mainly amorphous. After calcination at 750 °C, CeO_2 and rutile were detected besides $CeTi_2O_6$ at $x < 0.3$, but only $CeTi_2O_6$ was detected at $x = 0.3$. $CeTi_2O_6$ crystallized completely after calcination at 800 °C. At $x = 0.4$ or 0.5, both CeO_2 and $CeTi_2O_6$ existed. At $x = 0.6$, there was little amount of $CeTi_2O_6$, indicating that TiO_2 had entered the crystal lattice of CeO_2.

(2) The H_2 consumption of $Ce_xTi_{1-x}O_2$ (650 °C)(except $x = 0.1$) was greater than that of single CeO_2, and the valence of CeO_2 was the lowest (+3.18) at $x = 0.3$.

(3) $CuO/Ce_{0.3}Ti_{0.7}O_2$ calcined at 650 °C had the highest activity in NO + CO reaction, and the NO conversion reached 100% at reaction temperature of 300 °C. $Ce_{0.3}Ti_{0.7}O_2$ also began to crystallize at calcination temperature of 650 °C.

(4) The absorption centers of NO on $CuO/Ce_{0.3}Ti_{0.7}O_2$ catalysts were Cu^{+}, Cu^{2+}(I), Cu^{2+}(II) and Ce^{3+}, and the active components in NO + CO reaction were the Cu species (Cu^{2+}(I) and Cu^{+}) and the Ce species (Ce^{3+} and Ce^{4+}).

References

[1] H.C. Yao and Y.F. Yao, J. Catal. 86 (1984) 254.
[2] A.Trovarelli, C. Leitenburg and M. Boaro, Catal. Today 50 (1999) 353.
[3] D. Terribile, A. Trovarelli and J. Llorca, J. Catal. 178 (1998) 299.
[4] T. Masui, K. Fujiwara and Y. Peng, J. Alloys Comp. 269 (1998) 116.
[5] J.R. Gonzalez-Velasco, M.A. Gutierrez-Ortiz and J.L. Marc, Appl. Catal. B 22 (1999) 167.
[6] C.E. Hori, H. Permana and K.Y. Simon, Appl. Catal. B 16 (1998) 105.
[7] H. Vidal, J. Kaspar and M. Pijolat, Appl. Catal. B 27 (2000) 49.
[8] P. Formasier, J. Kaspar and M. Graziani, J. Catal. 167 (1997) 576.
[9] R. Lin, Y.J. Zhong and T.H. Wu, J. Rare Earths 20 (2002) 20.
[10] J. Rynkowski, J. Farbotko and R. Touroude, Appl. Catal. A 203 (2000) 335.
[11] X. Yan, K. Song and J. Wang, J. Rare Earths 16 (1998) 275.
[12] M. Luo, J. Chen and L. Chen, Chem. Mater. 13 (2001) 197.
[13] R. Brayner, D. Ciuparu and G.M. Cruz, Catal. Today 57 (2000) 261.
[14] A. Pruess and R. Gruehn, J. Solid State Chem. 110 (1994) 363.
[15] C.E. Bamberger, T.J. Haverlock and S.S. Shoup, J. Alloys Comp. 204 (1994) 101.
[16] A. Dauscher, P. Wehrer and L. Hilaire, Catal. Lett. 14 (1992) 171.
[17] R.D. Monte, P. Fornasiero, and J. Kaspar, Appl. Catal. B: Environ. 24 (2000) 157.
[18] G. Cordoba, M. Viniegra and J.L.G. Fierro, J. Solid State Chem. 138 (1998) 1.
[19] M.S.P. Francisco, P.A.P. Nascente and V.R. Mastelaro, J. Vac. Sci. Tech. 19 (2001) 1150.
[20] X.Y. Jiang, L.P. Lou, Y.X. Chen, X.M. Zheng, J. Mol. Catal. A 179(2003)193.